Measuring the accuracy of an ultrasonic heat meter with the MAX35101

By Jim Mitrosky

SIMULATION AND CORRELATION of flow-rate measurement in an ultrasonic heat-meter design is critical to the success of the heat-meter development process. Flow-rate measurement provides the designer with beneficial insight into the entitled accuracy of the heat-meter system measurement electronics, as well as a means of developing the individual product specifications. Without the knowledge of an expected level of performance for the electronic system used to measure the time-of-flight acoustic path in the meter spool body, the designer would be only guessing at the potential performance limits of the design. Once the simulations are completed, the meter's actual flow-rate accuracy can be measured using the MAX35101 Time-to-Digital Converter with Analog Front-End (AFE) and matching piezoelectric transducers mounted in a spool body with the same dimensions as those used in the simulation model.

Ultrasonic Time-of-Flight flow-measurement principle

A typical ultrasonic time-of-flight heat-meter spool body is depicted in figure 1.

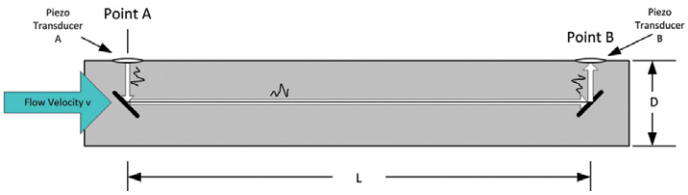

Fig. 1: Typical ultrasonic time-of-flight heat meter spool body.

The dimensions L and D are unique for every pipe size. The arrangement of the reflector surfaces within the flow spool body is also unique to every meter manufacturer. Consequently, the ultrasonic time-of-flight principle is based upon the time-of-flight of an acoustic signal in the water. The upstream time-of-flight is longer than the downstream time-of-flight, since the water velocity aids the acoustic signal in the downstream direction and impedes the acoustic signal in the upstream direction. This difference in time-of-flight can be exploited to determine the velocity of the flowing water.

The acoustic time-of-flight of an ultrasonic signal in the downstream direction is:

$$t_{A>B} = \frac{D/2}{C_O} + \frac{L}{(C_O + v)} + \frac{D/2}{C_O} \qquad (Eq.\,1)$$

The acoustic time-of-flight of an ultrasonic signal in the upstream direction is:

$$t_{B>A} = \frac{D/2}{C_O} + \frac{L}{(C_O - v)} + \frac{D/2}{C_O} \qquad (Eq.\ 2)$$

Where:
C_O is the speed of sound in water

v is the velocity of the water

Subtracting Equation 2 from Equation 1 and simplifying the results, followed then by solving for v, yields the velocity of the water:

$$v = \frac{(t_{B>A} - t_{A>B}) * C_O^2}{2 * L} \qquad (Eq.\,3)$$

The volumetric flow of the water is then simply calculated with knowledge of the cross-sectional area of the flow diameter of the spool body:

$$v_m = v * \frac{\pi * D^2}{4} \qquad (Eq.\,4)$$

This volumetric flow-rate measurement is the basis for determining the flow rate in a heat-meter system.

Flow-rate simulation of a typical ultrasonic ToF heat meter

Using a spreadsheet, the time-of-flight can be calculated and then converted to a volumetric flow rate using Equations 1 through 4. By simulating the time-to-digital converter electronics error of the time-of-flight measurement of the acoustic wave, plots of the entitled accuracy of the system can be created. Note that Equation 3 shows a dependency on the speed of sound in water, where C_Ois dependent upon the temperature of the water. Accurate temperature measurement of the water flow is needed by the heat meter so it can compute the energy consumed. If we assume that the water temperature is +70°C and can be measured accurately, the plot for the simulated flow rate for the typical ultrasonic time-of-flight heat meter shown above is depicted in figure 2.

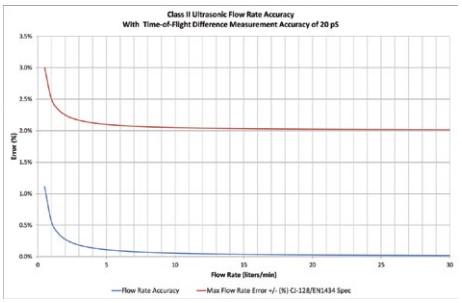

Fig. 2: Simulated flow-rate accuracy of the typical ultrasonic time-of-flight heat-meter spool body.

Notice from the plot of figure 2 that the simulated flow-rate accuracy, using the delta-time accuracy of the MAX35101 of 20ps

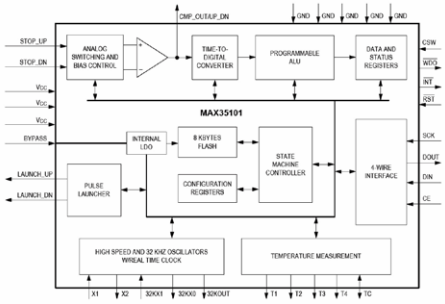

Fig. 3: Block diagram of the MAX35101 time-to-digital converter with analog front-end.

Jim Mitrosky is a Principal Member of Technical Staff at Maxim Integrated - www.maximintegrated.com

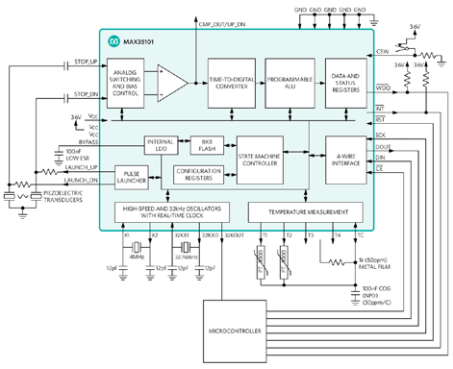

Fig. 4: Complete heat meter design using the MAX35101.

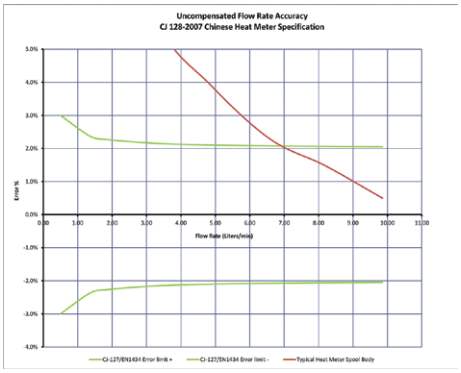

Fig. 5: Uncompensated flow-rate accuracy for the typical ultrasonic time-of-flight heat-meter spool body.

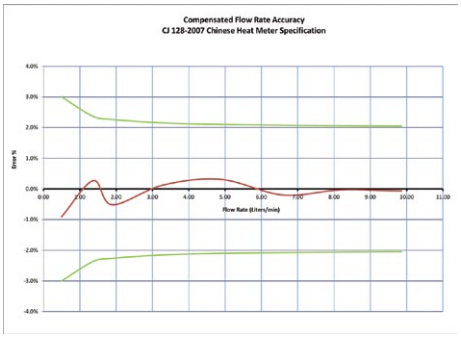

Fig. 6: Compensated flow-rate accuracy for the typical ultrasonic time-of-flight heat-meter spool body.

of time-of-flight, exceeds the specification error bars by a significant margin. This simulation depicts the entitled flow-rate accuracy without the effects of flow turbulence and mechanical design limitations in the spool body. Any additional error in the system would add to the error shown in this plot. The main sources of that additional error include the effects of flow turbulence and mechanical design limitations in the spool body. The actual flow-rate measurement accuracy is limited and can only approach that of the simulation model with sample averaging, totalizing, and multipoint flow calibration.

The typical ultrasonic time-of-flight heat meter incorporating the MAX35101 is then connected to a water-flow system so that the IC can actually measure flow rate through the meter spool body. The block diagram for MAX35101 is shown in figure 3.

The meter itself is composed of a MAX35101 mated to a low-power microcontroller, a battery, the spool body, and the transducers. The MAX35101 can take automatic differential time-of-flight measurements.

Its Early Edge Detect feature allows the MAX35101 to measure zero-crossing data consistently between measurements. With its ability to measure the temperature of the water, the time-of-flight data can compensate for the differences in the speed of sound in water at different temperatures. The MAX35101 offers an event timing mode that is configurable and runs cyclic algorithms to minimize microprocessor interactivity and increase battery life.

The real-time clock (RTC) provides one programmable alarm and watchdog functionality. A simple opcode-based 4-Wire SPI interface allows any microcontroller to effectively configure the device for its intended measurement. On-board user flash allows the MAX35101 to be nonvolatile configurable, and provides nonvolatile energy use data to be logged.

A full system diagram of a reference Heat Meter using the MAX35101 is shown in figure 4.

Raw flow-rate data can be taken with the system of Figure 4. This raw data is depicted in figure 5. The plot represents a data set that comprises multiple samples taken at fixed flow-rate intervals. Each flow-rate interval is sampled 50 times to obtain a statistical distribution of the measurement error in the spool body. Notice that this plot is focused on the low-rate region from 0 to 10 liters per minute. The error that is revealed by this plot is sourced from the effects of flow turbulence and mechanical design limitations in the spool body. The accuracy of the MAX35101 is not a contributing factor to this error. The accuracy of the plot of figure 5 can be increased by applying a typical multipoint compensation curve to the raw data. The data needed to produce the compensation curve is gathered from a highly accurate flow-rate reference. The National Institute of Standards and Technology (NIST) in the United States uses a gravimetric reference system. This is a weigh system with collection tank and a flow-diverting device.

PICO
SURFACE MOUNT
(and thru-hole)
Transformers
& Inductors
Size
does
matter!

from
low-
profile
.18"ht.
• Audio Transformers
• Pulse Transformers
• DC-DC Converter Transformers
• MultiPlex Data Bus Transformers
• Power & EMI Inductors
ISO9001:2000
AS 9100 REV B
See Pico's full Catalog immediately
www.picoelectronics.com
PICO Electronics,Inc.
143 Sparks Ave. Pelham, N.Y. 10803
E Mail: info@picoelectronics.com
Pico Representatives
Germany
ELBV/Electronische Bauelemente Vertrieb
E-mail: info@elbv.de
Phone: 0049 89 4602852
Fax: 0049 89 46205442
England
Ginsbury Electronics Ltd.
E-mail: rbennett@ginsbury.co.uk
Phone: 0044 1634 298900
Fax: 0044 1634 290904

This device is the part of the calibration system that directs the flowing water into the collection tank while triggering a clock to determine the collection time. The water collected can be determined in terms of volumetric or gravimetric units. The calibration technique used for the set of measurements taken to obtain the multipoint compensation curve is based upon a reference flow meter that is traceable to this NIST gravimetric reference system.

Calibration of each meter is unique, and usually performed by the meter manufacturer before shipment to the end customer. A 10-point compensation curve is applied to the plot of figure 3 to yield the plot of figure 6. Notice in figure 6 that the flow-rate accuracy is better than ±1% down to 0.5 liters per minute of flow rate. By comparing the plot of figure 6 to the plot of figure 2, it can be seen that the accuracy of the meter can be made to reflect the accuracy of the MAX35101.

Power routing in analogue design

By Keith Sabine

KEITH SABINE, product manager at EDA firm Pulsic, discusses the issues around power net routing for analogue blocks within integrated circuits.

Automating analogue design requires that constraints such as symmetry and matching, noise coupling, and the use of shielding be part of the automated flow. Commercial routers capable at the device level can handle some of these types of constraints, but handling power net routing is typically done by planning manually.

In the digital world, power distribution methodology is much easier. With row-based, standard cell placement and routing (P&R), and the availability of relatively many metal layers, power rings and meshes can be easily generated automatically. True, this can become more complicated as designers seek to use less power by using power switches and have multiple voltage domains, but there are well established EDA tools to help designers analyze and optimize power distribution schemes.

For small analogue IP blocks, power routing can often be relatively simple. A common approach is to start with a "template" cell defining the desired block size, pin positions, and VDD/VSS rails, typically at the top and bottom of the block. However, even for relatively simple blocks, the power hookup to devices has generally been done manually. Actually, there is no reason why a mesh-type structure can't be used; for example, two layers are shown in figure 1, which shows VDD/VSS rails at the top and bottom of the block with an irregular H-shaped mesh in the centre. The key to achieving this is the ability to place and route devices, signal nets, and power nets simultaneously. Device S/D pins can directly strap to the power mesh to give a clean routing style.

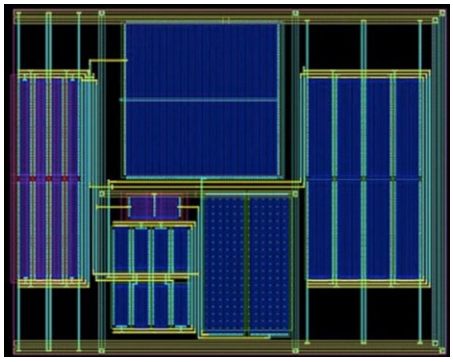

Fig. 1: Automated power routing mesh for an analogue block.

Widths of power tracks need to be considered carefully for analogue layout. As geometries get smaller, tapering of power nets may be required since uniform-width nets may be too wide for individual transistor tap-offs, but too narrow due to electromigration rules for higher current portions of the nets. In this case, careful consideration of current flow is required in order to size the net segments appropriately. Simulation results of transistor pin currents are required here in order to accurately model the current requirements of the power nets (and potentially the signal nets, too).

Another common approach is to use combined power and guard rings/rails. The "variable mesh" approach can also be used here, although it becomes more complex as guard rings require single layer (i.e., wrong way) preferred directions. Again, device S/D pins can tap into guard rings to simplify local power routing.

A further development would be to support hierarchical power routing, where power pins on the lower-level blocks strap into the higher-level cells' mesh. Once again, actual net widths need to be computed accurately for this approach.

As can be seen, automated analogue routing presents challenges compared to digital power distribution. However, with new techniques and methodologies, automation is possible, and the goal of speedier design iterations can be achieved, enhancing productivity.

Keith Sabine is Product Manager for Analogue Solutions at Pulsic Ltd – www.pulsic.com

Oscilloscope engine plugs into portable Apple products

This month, Oscium is giving away three of its iMSO-204L dual analogue iOS oscilloscopes, worth USD400 each. Designed with native Lightning compatibility, the iMSO-204L transforms the iPad, iPhone, and iPod touch into an ultra-portable, two-channel oscilloscope. Since Apple changed its connector, Oscium has been working to bring native compatibility to its customers. The third generation of handheld engineering tools from Oscium, the iMSO-204L is the solution to the connector change, featuring two analogue and four digital channels, capable of 50 MSPS at a 5MHz bandwidth, and with a resolution varying from 200ns/div to 10s/div. The iMSO2 software supports single-shot waveform capture, pause and zoom through the touchscreen and AirPlay compatibility (so the oscilloscope display can be mirrored onto compatible projectors). The iMSO2 software is free in the Apple App Store, it is compatible with the iPhone 5C, iPhone 5S, iPhone 5, iPad Mini, iPad Air, iPad 4 and iPod touch [5th generation].

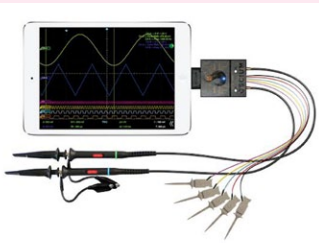

Check the reader offer online at www.electronics-eetimes.com